Biogeosciences Discuss., 12, 2021–2061, 2015
www.biogeosciences-discuss.net/12/2021/2015/
doi:10.5194/bgd-12-2021-2015

Biogeosciences
Discussions
Open Access

Understanding emissions of ammonia from buildings and application of fertilizers: an example from Poland

M. Werner[1,2], C. Ambelas Skjøth[1], M. Kryza[2], and A. J. Dore[3]

[1]National Pollen and Aerobiology Research Unit, University of Worcester, UK
[2]Department of Climatology and Atmosphere Protection, University of Wroclaw, Poland
[3]Centre for Ecology and Hydrology, Edinburgh, UK

Received: 5 December 2014 – Accepted: 5 January 2015 – Published: 30 January 2015

Correspondence to: M. Werner (m.werner@worc.ac.uk)

Published by Copernicus Publications on behalf of the European Geosciences Union.

Abstract

A Europe-wide dynamic ammonia (NH_3) emissions model has been applied for one of the large agricultural countries in Europe, and its sensitivity on the distribution of emissions among different agricultural functions was analysed by comparing with observed ammonia concentrations and by implementing all scenarios in a chemical transport model (CTM). The results suggest that the dynamic emission model is most sensitive to emission from animal manure, in particular how animal manure and its application on fields is connected to national regulations. In contrast, the model is most robust with respect to emission from buildings and storage. To incorporate the national regulations, we obtained activity information on agricultural operations at the sub-national level for Poland, information about infrastructure on storages, and current regulations on manure practice from Polish authorities. The information was implemented in the existing emission model and was connected directly with the NWP calculations from the Weather Research and Forecasting model (WRF-ARW). The model was used to calculate four emission scenarios with high spatial (5 km × 5 km) and temporal resolution (3 h) for the entire year 2010. In the four scenarios, we have compared the Europe-wide default model settings against (1) a scenario that focuses on emission from agricultural buildings, (2) the existing emission method used in WRF-Chem in Poland, and (3) a scenario that takes into account Polish infrastructure and agricultural regulations. The ammonia emission was implemented into the CTM FRAME and modelled ammonia concentrations was compared with measurements. The results suggest that the default setting in the dynamic model is an improvement compared to a non-dynamical emission profile. The results also show that further improvements can be obtained on the national scale by replacing the default information on manure practice with information that is connected with local practice and national regulations. Implementing a dynamical approach for simulation of ammonia emission is a viable objective for all CTM models that continue to use fixed emission profiles. Such models should handle ammonia emissions in a similar way to other climate-dependent emissions (e.g. bio-

genic volatile organic compounds). Our results, compared with previous results from the DEHM and the GEOS-CHEM models, suggest that implementing dynamical approaches improves simulations in general, even in areas with limited information about the location of the agricultural fields, livestock and agricultural production methods such as Poland.

1 Introduction

Ammonia is mainly emitted to the atmosphere from agricultural operations (Bouwman et al., 1997), but also from natural sources (Riddick et al., 2014). Ammonia is the main alkaline gas in the atmosphere (Hertel et al., 2012) and is responsible for neutralizing acids (sulfuric and nitric acid) formed through the oxidation of sulfur dioxide (SO_2) and nitrogen oxides (NO_x) (Seinfeld and Pandis, 2006). This leads to creation of ammonium (NH_4^+) salts, which are incorporated in atmospheric aerosols (Banzhaf et al., 2013; Reis et al., 2009). The emission of NH_3 makes a major contribution to the formations of particulate matter (PM_{10} and $PM_{2.5}$) (de Meij et al., 2009; Werner et al., 2014a), accounting for up to 50 % of the total mass of $PM_{2.5}$ (Anderson et al., 2003). As such, ammonia-containing aerosols are a very important component in regional and global aerosols processes (Xu and Penner, 2012). There is a direct climate penalty on ammonia emission (Skjøth and Geels, 2013), mainly because the volatilization potential of ammonia nearly doubles for every 5 °C temperature increase (Sutton et al., 2013). In the fifth report of the IPCC, ammonia emission is highlighted as an important component with a considerable feedback effect on climate and air quality that still remains to be understood (IPCC, September 2013). There is therefore a need to improve the descriptions of ammonia emission models and advance the level of input data to these models (Flechard et al., 2013; Guevara et al., 2013; Wichink Kruit et al., 2012) and thus use them with chemistry transport models. Ideally, this improved approach should directly use results from climate or numeric weather prediction (NWP) models (Sutton

BGD
12, 2021–2061, 2015

et al., 2013) because the fluxes of ammonia with the surface are directly and non-linearly related to meteorology (Baklanov et al., 2014).

Ammonia affects the acidification of soils that arises from the deposition of N from the atmosphere (Sutton et al., 2009; Theobald et al., 2009). The two governing processes for nitrogen deposition are wet deposition of ammonium-containing aerosols and dry deposition of ammonia (Bash et al., 2013; Hertel et al., 2012). Ammonia also contributes to the eutrophication of terrestrial ecosystems and surface waters and the development of a lower tolerance to stress in woodland and forests (Sutton et al., 1998, 2009). This eutrophication leads to loss of plant diversity in a wide range of habitats (Emmett, 2007; Jones et al., 2011a; Stevens et al., 2004). Nitrogen deposition exceeds the critical loads in most European countries, such as France (van Grinsven et al., 2012), the Netherlands (Jones et al., 2011b), Belgium (Jones et al., 2011b), Germany (Nagel and Gregor, 2001) and Poland (Hettelingh et al., 2009; Kryza et al., 2013a). The regions with the highest nitrogen deposition are the areas with intense agricultural production, high ammonia emission and correspondingly high deposition of ammonia-containing compounds (Hertel et al., 2012; Wichink Kruit et al., 2012). The calculation of maps of critical load exceedance require chemical transport models (CTMs) to generate estimates of nitrogen deposition (Flechard et al., 2013). These exceedance maps generally require high spatial and temporal resolution in the atmospheric models (Geels et al., 2012; Mues et al., 2014), and it has been shown that this requires detailed information on emissions from different agricultural operations (e.g. Skjøth et al., 2011). These operations also rely on national legislations on manure management (e.g. Gyldenkærne, 2005) and regional husbandry methods (e.g. Skjøth et al., 2011), as well as prevailing crops and use of mineral fertilizer (Gyldenkærne, 2005; Misselbrook et al., 2006). This information can be obtained from agricultural databases in countries like Denmark (e.g. Gyldenkærne, 2005), the Netherlands (van Pul et al., 2008) and the UK (Hellsten et al., 2008), but has so far not been available in countries with substantial ammonia emissions such as France, Italy and Poland. Simplified approaches to agricultural production methods (activity data) have therefore

BGD
12, 2021–2061, 2015

been applied in existing models that aim at making Europe-scale calculations (Skjøth et al., 2011), which will decrease the quality of the results. It has therefore been highlighted that there is a need to obtain national and detailed activity data and integrate this information into models (Flechard et al., 2013).

The aim of this paper is to obtain activity information on agricultural operations at the subnational level for one of the largest agricultural countries in Europe, Poland, and implement these data within an existing ammonia emission model (Skjøth et al., 2004, 2011). We will connect the model directly with the NWP calculations from the WRF model (Skamarock and Klemp, 2008) according to the suggestion of Sutton et al. (2013) on a model grid that is identical to the WRF-Chem model for Poland (Werner et al., 2014b). With this we will compare the Europe-wide default settings (Skjøth et al., 2011) against (1) a scenario that focuses on emissions from agricultural buildings, (2) the existing method used in WRF-Chem over Poland, and (3) a scenario that takes into account Polish infrastructure and less regulation compared to Denmark. We will test all four scenarios for a full year with a simplified CTM in order to minimize the computational penalty with WRF-Chem and compare the results from our four scenarios with related results that have been obtained for Denmark (Skjøth et al., 2011), Germany (Skjøth et al., 2011) and France (Hamaoui-Laguel et al., 2014).

2 Methodology

2.1 Emission model

NH_3 emissions have been calculated with a dynamic model originally developed for Denmark. The fundamentals of the model are provided by Gyldenkærne (2005), Skjøth et al. (2004) and Skjøth et al. (2011). The general idea behind the emission model is to use the gridded annual total NH_3 emissions (data described in the next section) and to use available activity data to make a disaggregation of the gridded annual totals into specific agricultural sectors with a similar emission pattern. The emission from

BGD
12, 2021–2061, 2015

each sector then uses a parameterization that depends on both the volatilization as a function of meteorology and the temporal pattern of the activity. This creates a set of additive continuous emission functions, denoted as Fct_i, typically with a time resolution of 1 or 3 h. The methodology allows for either full agreement with national annual official emissions (Skjøth et al., 2011) or freely fluctuating emissions due to meteorology, where the freely fluctuating emissions can be either larger or smaller compared to official estimates (Skjøth and Geels, 2013). The emission parameterization consists of 16 additive continuous functions (Table 1), describing emission from animal houses and storage (3 functions), application of manure and mineral fertilizer (7 functions), emission from crops (4 functions), grazing animals, ammonia treatment of straw, and road traffic. The applied functions were originally derived for Danish conditions and presented in Skjøth et al. (2004), but Skjøth et al. (2011) suggest that the majority of the functions may be directly applicable for a large part of Europe. Default values were therefore implemented for many European countries. Several of the underlying studies for producing parameterizations, such as the applied growth model (Olesen et al., 1995) and the farm surveys by Seedorf et al. (1998a, 1998b), are based on Europe-wide studies and are considered appropriate for large geographical regions (Skjøth et al., 2011), while the parameterizations for manure application may need adaptation to national regulation, which is known to change over time (Skjøth et al., 2008).

The functions for emission from stables and manure storage are defined in Eq. (1), and the temporal profile of emission depends on air temperature and wind speed in a given grid cell:

$$\mathrm{Fct}_i = \frac{E_i(x,y)}{\mathrm{Epot}_i(x,y)} \times (T_i(x,y))^{0.89} \times (W_i(x,y))^{0.26} \quad i = [1;3]. \tag{1}$$

Index i refers to functions 1–3 and x and y refer to the coordinate in the east–west direction and south–north direction. Fct_1 refers to animal houses with forced ventilation, Fct_2 refers to open animal houses, and Fct_3 to manure store. $E_i(x,y)$ is the emission input into the model and $\mathrm{Epot}_i(x,y)$ is the emission potential scaling factor for a given

BGD
12, 2021–2061, 2015

grid cell. The emission potential is used to scale the annual emission up/down in accordance with the officially reported value. Input emission data for the Poland domain were obtained according to the procedure described in Sect. 2.1.1. $T_i(x,y)$ is the temperature in either animal houses or at the surface of the manure storage, and W is either the ventilation inside the building or the 10 m wind speed above the storages. The emission potential is approximated by the 2 m air temperature, provided by the WRF-ARW model and a simple parameterization for temperatures and ventilation in stable systems (Gyldenkærne, 2005). The WRF-ARW model configuration and evaluation is provided in the following sections.

Functions Fct_4–Fct_{15} are related to plant growth and include emissions from both plants and due to applications of fertilizer and manure (Table 1). Functions 4 to 15 depend on both air temperature and wind speed. The temporal variations for these activities have therefore been parameterized by the Gauss functions (Eq. 2).

$$\mathrm{Fct}_i = \left(W_{\mathrm{corr}} \times T_{\mathrm{corr}} \frac{E_i(x,y)}{Epot_i(x,y)}\right) \times \frac{e^{\left(\frac{(t-\mu_i(x,y))^2}{-2\sigma_i^2(x,y)}\right)}}{\sigma_i\sqrt{2\pi}} \quad i = [4;15] \tag{2}$$

Here, μ_i is the mean value for the parameterized distribution understood as the time of the year when the Gauss function obtains its maximum value. σ_i is the spread of the Gauss function. W_{corr} and T_{corr}, which are related to meteorological parameters – wind speed and temperature, are given in Gyldenkærne (2005). The emission from plants is only included in the inventories for a few countries (e.g. Gyldenkærne, 2005) and can in principle be calculated online in a chemical weather forecast model (e.g. Sutton et al., 2013) by using a mechanism that describes the bi-directional flux (Massad et al., 2010). Emissions from plants were therefore not included here.

2.2 Emissions input data and scenarios

The spatial pattern of NH_3 agricultural emission for Poland for the year 2010 was prepared using the methodology proposed by Dragosits et al. (1998), which is imple-

BGD
12, 2021–2061, 2015

Understanding emissions of ammonia from buildings and fertilizer use

M. Werner et al.

mented in several atmospheric model systems over the UK (e.g. Oxley et al., 2013). Data on the animal number and fertilizer consumption, provided by the Polish National Statistical Office, were combined with the national emission estimates (KOBIZE 2013) and spatially allocated with using gridded data from the Corine Land Cover map (European Commission, 2005). Data on animal numbers were available at commune level and fertilizer consumption at province level. Detailed information about the calculation methodology used for Poland is described in Kryza et al. (2011). The annual NH_3 emissions were gridded to a spatial resolution of 5 km × 5 km to be in accordance with the mesh in the meteorological model (Fig. 1).

The annual gridded NH_3 emissions were then used to construct four scenarios, termed DEFAULT (1), NOFERT(2), FLAT(3) and POLREGUL(4) (Table 2). For the POLREGUL scenario the information on Polish infrastructure and management methods was obtained from the IIASA review for the Danish and Polish area (Klimont and Brink, 2004). Firstly, both countries have a ban on application of manure and mineral fertilizer before 1 March. Secondly, the manure storage capacity in Poland is about 3 months, compared to 7–9 months in Denmark. This means that farmers in Poland need to apply manure during spring, summer and autumn. In Poland between 10 and 20 % of husbandry manure (only slurry) is applied to grassland, which covers about 25 % of the agricultural area. Poland does not have a detailed nitrogen quota system at the field level like Denmark does, and the Polish regulation does not contain definitions of manure-N efficiency. The Danish regulations force farmers to apply most of the mineral fertilizer and husbandry manure to growing crops, and there is a strict limit on how much manure and mineral fertilizer is allowed to be added to each field in Denmark (Skjøth et al., 2008). A consequence is that a limited amount of mineral fertilizer is used in Denmark and that the majority (90 %) is applied to growing crops (April–May) and the remaining part to grassland (summer). This is not the case in Poland, where there is a larger consumption of mineral fertilizer. Assuming that all fields in Poland receive sufficient fertilizer (manure and mineral) without an upper limit forced by regulation, a consequence is that as much manure as possible will be used early in the

BGD
12, 2021–2061, 2015

season and that the majority of the mineral fertilizer will be used on grasslands during summer (especially June, July and August) as there is a ban on applying mineral fertilizer to meadows and pasture after 15 August. Therefore the simple assumption is that all fields will have equal amounts of manure and mineral fertilizers during spring and summer (Table 3, Poland scenario). Finally, the regulations in Poland allow farmers to apply manure to fields throughout October, which is not allowed in Denmark. A consequence is that the timing of this autumn application, when the farms empty their storages, has its peak 2–4 weeks later than in Denmark. We have therefore chosen ordinal day number 290 (counted from the beginning of January each year, in our study 2010) as the default peak time for this activity in Poland.

2.3 Meteorological input data – WRF-ARW model configuration and model performance

The Advanced Research WRF model was used with three one-way nested domains (Skamarock and Klemp, 2008). The outer domain (131 × 131 grid points) covers Europe with a horizontal resolution of 45 km × 45 km. The intermediate domain covers the area of central Europe with a resolution of 15 km × 15 km (94 × 94 grid points). The innermost domain (194 × 194 grid points) covers the area of Poland at 5 km × 5 km resolution. Meteorological data from the innermost domain are used in this study. Vertically, the domains are composed of 35 terrain-following hydrostatic-pressure coordinates, with the top fixed at 10 hPa. The simulation was driven by the NCEP final analysis available every 6 h with $1.0^{\circ} \times 1.0^{\circ}$ spatial resolution. Analysis nudging was applied for the first two domains.

The model uses the same configuration of physics as presented by Kryza et al. (2013b), including the Goddard microphysics scheme (Tao et al., 1989), Yonsei University planetary boundary layer scheme (Hong et al., 2006), MM5 similarity surface layer, and RRTMG and RRTM schemes for short- and longwave radiation (Iacono et al., 2008; Mlawer et al., 1997). The Kain–Fritsch cumulus scheme is applied for the first two domains (Kain, 2004). For the innermost domain, cumulus convection is explicitly resolved.

Because the WRF-ARW-derived spatial information on air temperature and wind speed is a key input for the emission model, the modelled meteorological data were extensively evaluated by comparison with the measurements. The measurements were available every 6 h from 69 meteorological stations located in Poland. The domain-wide error statistics were calculated and summarized with three error statistics: mean error (ME), mean absolute error (MAE) and index of agreement (IOA, unitless). The definitions of the aforementioned error measures are listed in the Supplement (Table 1). Air temperature at 2 m (T2) and wind speed at 10 m a.g.l. (W10), which are used by the dynamic model of ammonia emission, show good agreement with the measurements (Table 4). The air temperature is slightly underestimated, but the IOA is very close to 1.0. The wind speed is slightly overestimated, with the ME > 0.

2.4 The FRAME model

The standard version of the Fine Resolution Atmospheric Multi-pollutant Exchange (FRAME) model provides information on the annual mean oxidized sulfur and oxidized and reduced nitrogen atmospheric air concentrations and deposition. A detailed description of the FRAME model is given in Singles et al. (1998), Fournier et al. (2004), Dore et al. (2006) and Vieno et al. (2010). Details on the model configuration for Poland can be found in Kryza et al. (2010, 2012) and Werner et al. (2014a). FRAME is a Lagrangian model which describes the main atmospheric processes in a column of air moving along straight-line trajectories following specified wind directions. The model consists of 33 vertical layers of varying thickness, ranging from 1 m at the surface to 100 m at the top of the domain. As such the FRAME model is designed for studies where processes on the local scale and landscape scale will be governing (e.g. ammonia emissions) and have a simplified treatment of long-distance transport and associated chemistry. Trajectories are advected with different starting angles at a 1° resolution using directionally dependent wind speed and frequency roses. Concentrations at the boundary of the model domain are calculated with the FRAME-Europe model, which is a model similar to FRAME but which runs for the whole of Europe on the EMEP grid at 50 km × 50 km resolution. For this study the model was adapted to run and provide results at monthly resolution. Monthly wind roses were developed from the WRF data using a method similar to that described by Dore et al. (2006). Information on rainfall for FRAME was calculated by using observed data from 210 rainfall sites in Poland. Geographically weighted regression kriging, with elevation used as an independent explanatory variable (Szymanowski et al., 2013), was used here to produce a 5 km × 5 km gridded data set that matches the meteorological grid from the WRF model.

FRAME was run four times for each month. Simulations for 1 month differ in the emission scenario, and are described in Table 2 (Sect. 2.2).

2.5 Measurements of ammonia (NH_3) and ammonium (NH_4^+) air concentrations and backward trajectories from the WRF-ARW model

Verifying observations are obtained from stations within the EMEP network (Aas et al., 2012). Four EMEP stations that measure daily air concentrations of gaseous ammonia and aerosol ammonium ($NH_3 + NH_4^+$) and NH_4^+ are available for Poland: PL02 Jarczew, PL03 Śnieżka and PL04 Łeba, PL05 Diabla Góra (Fig. 1). Three of these EMEP stations are located in specific geographical areas (Łeba – at the coast in the north; Śnieżka – the highest peak in the Sudety Mountains, SW Poland; and Diabla Góra – in a large forestland, NE Poland). These areas contain limited or even no agricultural activity. Only Jarczew station, located in central-eastern Poland, is located in an agriculture area, and is therefore best suited for validation of the model results. One additional site from the NitroEurope network provided measured monthly ammonia concentration. This site, Rzecin, is located in a wetland area surrounded by forests with full coverage of woodland within the nearest 1 km. Land cover outside this woodland is mainly agricultural, and with the highest ammonia emissions in Poland.

Error statistics ME, MAE and R for modelled and measured NH_3 concentrations were presented for each site individually, and mean statistics based on five stations were

BGD
12, 2021–2061, 2015

calculated for the entire year and for the periods with (March–October) and without application of manure (January, February, November, December). The definitions of the error measures are listed in the supplementary material (Table 1).

Additionally, for Jarczew, the 3-hourly emissions from the dynamic model were aggregated into daily values and plotted with average daily concentrations from the station. The daily observations and aggregated model calculations were then sorted in two groups: (1) a group with high concentrations of NH_3 that were not simulated by the emissions model, and (2) the remaining days. Group 1 was then investigated in detail using air mass trajectories calculated with WRF-ARW data. RIP version 4.5 (Stoelinga., 2008) was used to get 36 h backward trajectories for the Jarczew station. Six trajectories were run for each day with an episode from group 1, once every 6 h and for the receiving heights 250 and 750 m. Each episode was then analysed with respect to potential atmospheric transport from neighbourhood regions with high ammonia emissions.

3 Results

The results are organized as follows: first the annual ammonia emission and results from the POLREGUL option of the dynamic model for Poland are described. In the second subsection, FRAME model concentrations from four runs (DEFAULT, NOFERT, FLAT and POLREGUL) are presented and compared with measurements. Finally, the relationship between the dynamically modelled emissions and measured concentrations for one selected station is presented.

3.1 NH_3 emission in Poland in 2010

Total ammonia emission (sum for the total area of the country) in Poland in 2010 was 270 Gg. The highest annual emissions are in the central part of the country, and locally exceed 35 kg ha^{-1} year^{-1} (maximum 45 kg ha^{-1} year^{-1}, Fig. 2). These are areas with

BGD

12, 2021–2061, 2015

agricultural activity contributing to the majority of NH_3 emissions in Poland. The NH_3 emissions are in the range of 1 to 10 kg ha^{-1} year^{-1} over 70 % of the area of the country. The lowest emissions are in the west, north-west and south-east, where agricultural activity is less intense and large areas are covered with forests.

From analysis of the monthly totals of NH_3 emissions (Fig. 2) it can be seen that April is the month of highest emission for both the DEFAULT and POLREGUL model runs. In the case of the DEFAULT run, about 40 % of the annual emission is related to this month and minor emission peaks appear in March, July and September. For the POLREGUL scenario the April peak is lower by about 40 % in comparison to DEFAULT, and the increased emission also appears in July and October (Fig. 2). Generally, there was higher emission in the period with average monthly temperature above 5.0 °C.

The seasonal variation of emission (POLREGUL run) for different agricultural categories for the Jarczew station is shown in Fig. 3. In April, which is also the month with the highest ammonia emission for the total area of Poland, three functions have their highest values. At this time, the peaks are observed for applications of manure on bare soils and application of fertilizers and manure on crops. Ammonia-treated straw (Fct_{15}) is responsible for high ammonia emission in summer, whereas the autumn peak of emission (end of September, October) is mainly related to application of manure. Emission related to livestock is dominated by Fct_1 because of large-scale farming of pigs in Poland (37 cattle and 99 pigs per 100 ha of agricultural land, GUS 2010). Due to meteorological conditions (temperature), their contribution is doubled in the summer season in comparison to winter.

The spatial distribution of ammonia emission for selected days (sum of emission between hours 12:00 and 15:00 UTC for the 15th day of a month) is presented in Fig. 4. The 3-hourly averages for the total area of Poland are equal to 0.5, 8.0, 3.0 and 2.7 g ha^{-1} in February, April, June and September, respectively. The maximum values are observed in April in the central part of the country, where they reach 50 g ha^{-1}.

For the three selected locations (names of the locations are taken after the nearest towns, marked in Fig. 1) in Poland – Wrocław (south-west), Suwałki (north-east) and close to Leszno (central west) – hourly emissions for the selected period (from March to May) are shown in Fig. 5. Two of these locations represent the areas of the longest (Wrocław) and the shortest (Suwałki) growing season in Poland. The spring increase in emission appears first in Wroclaw (middle of March) and then almost 4 weeks later in Suwałki. Leszno is located in the area with the highest ammonia emissions in Poland. There is a large day–night emission variability due to diurnal variability in air temperature and wind speed.

3.2 NH_3 concentration calculated with the FRAME mode

The spatial distribution of modelled NH_3 concentration from the POLREGUL scenario for February, April, June and September is illustrated in Fig. 4. The highest concentrations are in the agricultural areas in the central part of Poland, with maximum values equal to 1.32, 26.0, 16.5 and 9.2 $\mu g\,m^{-3}$ for February, April, June and September, respectively. High spatial correlation (≥ 0.9) between the modelled ammonia emission and FRAME ammonia concentration (Fig. 4.) was calculated for each month.

Time series and error statistics of modelled (DEFAULT, NOFERT, FLAT, POLREGUL) and measured NH_3 concentrations are presented in Fig. 6 and Table 5. For most sites (Rzecin, Jarczew, Łeba and Śnieżka), R and MAE are best for the NOFERT and POLREGUL runs. The best performance was obtained for Jarczew and Rzecin. For each station the DEFAULT run calculates that the concentrations peak in April, which is not present in the measurements or is much lower than observed (Jarczew, Rzecin). Application of Polish regulations in the dynamic model has improved the results most significantly in comparison to DEFAULT for Rzecin and Jarczew. Jarczew is the only station located directly in an agricultural area, whereas Rzecin is under the influence of an agricultural region with the highest ammonia emission in Poland. The poorest performance for each model run is for Diabla Góra, for which the measured time series has a totally different pattern in comparison to the other sites. High measured concentrations for this station are obtained in late autumn and in the winter months.

BGD
12, 2021–2061, 2015

For three model runs (DEFAULT, NOFERT, FLAT), correlation coefficients are lowest for the summer period in comparison to the entire year (Table 6), whereas the summer period has the highest correlation coefficients for the POLREGUL scenario. The POLREGUL scenario therefore improved the results significantly in comparison to DEFAULT for summer period – the correlation coefficient increased from 0.21 to 0.73 and MAE decreased from 0.83 to 0.68.

3.3 Comparison of daily emissions with measured concentrations and backward trajectories case study

Due to the high spatial correlation between ammonia emission and concentration (Fig. 4), we looked for the relationship between the dynamically modelled emissions and measured concentrations for Jarczew station (Fig. 7). The main peaks in emissions (April, September) are reflected in the concentration data. There are also some peaks in concentrations (e.g. end of February, beginning of June and end of October) which are not resolved by the emission model. These could suggest the limitations of the emission model, or could be related to meteorology which has resulted in the transport of ammonia from neighbouring areas. Backward trajectories, for the mentioned high concentration episodes (end of February, beginning of June and end of October), were calculated with the RIP tool (Fig. 8) in order to check whether it is possible to connect these observed peaks in concentrations with atmospheric transport of ammonia. We have found that for these episodes the trajectories have a similar pattern – transport from the south or south-west sector. The air masses that reached Jarczew during these episodes had passed areas with high ammonia emissions in comparison to the local area surrounding the station.

BGD
12, 2021–2061, 2015

4 Discussion and conclusion

The temporal and spatial variability of ammonia emission has been analysed over Poland with four scenarios: DEFAULT (matches the Europe-wide default settings in the ammonia emission model; Skjøth et al., 2011), NOFERT (excludes application of manure and mineral fertilizer), FLAT (the existing emission method (no temporal variations) used in WRF-Chem over Poland) and POLREGUL (takes into account Polish infrastructure and current and less regulation compared to DEFAULT). The emissions were then implemented in the FRAME model for a fast response on simulating the effect of the scenarios in relation to atmospheric chemistry. The results show that, in general, the model simulations were improved by applying a dynamical model and using Europe-wide (default) settings instead of using a fixed emission profile. However, if Polish infrastructure and national regulation is incorporated into the model, much better results are achieved for agricultural areas.

The model results show large differences in emissions between months, as well as between day and night. This is due to increased volatilization of ammonia caused by increased temperatures (Eqs. 1 and 2) and emissions from animal and mineral fertilizer that are applied over short time periods during spring, summer and autumn (Eq. 2). Taking into account the entire area of the country, the highest emission is obtained during spring (especially in April). The spring emission peak (and corresponding concentrations) is mainly related to the application of fertilizers and manure, which is clearly illustrated by comparing the POLREG and NOFERT simulations (Fig. 6). The sensitivity of the model to the application of manure is highlighted by the large difference between the DEFAULT and POLREGUL scenarios. In April the emission is 40 % lower in the POLREGUL scenario than in the default scenario. This is not surprising, as previous results have shown that national regulation can cause emissions from manure to increase by more than 100 % in spring and decrease during summer to less than 10 % (Skjøth et al., 2008). The dynamic model predicts the spring peak in emission to start in south-west Poland and then progressing to the rest of the country (Fig. 5).

BGD
12, 2021–2061, 2015

South-west Poland has the longest growing season (Żmudzka, 2012) and is the area where farmers initiate their field activities in Poland. In this region, field work, including application of fertilizers or manure, can start earlier than in other regions of the country. This aspect of a northward "northward-progressing ammonia plume" due to spring application is therefore very well captured by the model and has also been implemented in the GEOS-CHEM model (Paulot et al., 2014) and DEHM (Skjøth et al., 2011).

Major NH_3 emission peaks modelled for the Jarczew agricultural station are also observed in NH_3 concentration measurements. However, some peaks in concentrations are not reflected in the emission data. As suggested by Asman et al. (1998) and Fowler et al. (1998), atmospheric ammonia can be transported up to 100 km. According to Geels et al. (2012), the fraction of locally emitted NH_3 depositing locally is on the order of 15–30 % for a grid of 16 km × 16 km. In our study, the analysis of backward trajectories showed that increased concentrations can be related to transport of ammonia from neighbouring areas with high emission. A more thorough investigation on this scale requires more sophisticated modelling tools than FRAME, such as WRF-Chem.

FRAME is a relatively simple Lagrangian model and the results were found to be in good agreement with measurements for Poland (Kryza et al., 2011, 2012; Werner et al., 2014a). This enables us to run several scenarios for the entire year without a large computational overhead. Furthermore, the results with FRAME are considered good enough for this study on the emission patterns, as the obtained monthly correlation coefficients on the POLREGUL scenario are similar to the model results that are obtained with both DEHM (Skjøth et al., 2011) and the DAMOS system (Geels et al., 2012). In fact, the very high spatial correlation between ammonia emission and ammonia concentration (Fig. 4) suggests that, on a monthly basis, the governing process for ammonia concentrations is emission and only to a smaller degree atmospheric transport and transformation. The four scenarios show that focus on the agricultural practice, national regulations and the infrastructure (e.g. storage facilities) is a key challenge but very important for obtaining the best results. For Poland it was possible to obtain results for Danish and German sites that are almost as good as DEHM, despite the lack of detail about location of the agricultural fields and the location, amount and type of livestock in Poland. This suggests that similar improvements can be obtained for other European areas.

One of the sites (Diabla Góra) has an inverted time series in comparison to all other stations – the highest ammonia concentration appears in late autumn and in the winter months. Our calculations, which took into account only agricultural sources, were not able to catch peaks in this period. The Diabla Góra station is located in a large forested area called "Borecka Forest", surrounded by lakeland, with a small contribution of arable land in the region. Due to this location, high ammonia concentrations in this period may be related to natural sources. Open water areas (Barrett, 1998; Sørensen et al., 2003) and natural land areas (Duyzer, 1994) have been shown to emit NH_3. Emission of NH_3 from ecosystems are found to take place when the atmospheric NH_3 concentration is lower than the stomatal NH_3 compensation point (Mattsson et al., 2009), as a result of decomposing leaf litter, and due to cuticular desorption (David et al., 2009; Hansen et al., 2013). As suggested by Hansen et al. (2013), natural ammonia emission from deciduous forests should be considered as an emissions source which could be dynamically simulated with atmospheric transport models. Another factor that can cause an increase of ammonia concentrations could be evaporation from ammonium-containing aerosols. Ammonium chloride, ammonium nitrate and ammonium bisulfate are all formed from reversible processes in the atmosphere. Such processes can be more efficiently studied with models like WRF-Chem once they have been connected with a dynamical ammonia emission model. The dynamical approach has consistently provided good results for agricultural regions during the winter months, which is due to the large response to ammonia emission from agricultural buildings caused by outside temperatures. Implementation of this type of emission model into WRF-Chem will be a direct response to the suggestion by Sutton et al. (2013), and a direct coupling between ammonia emission, meteorology and chemistry and can address some of the challenges in the modelling of air pollution that have been highlighted (Baklanov et al., 2014).

For regional modelling of ammonia in Europe, the overall results suggest that it will be an advantage to move from a static to a dynamical approach. The Europe-wide default setting in the model given by Skjøth et al. (2011) can be expected to improve the results over large areas, but a better picture over Poland can be obtained if the values from Table 2 in Skjøth et al. (2011) are replaced with the values from our POLREGUL scenario. Further improvement on ammonia emissions is likely to be related to natural sources (Hansen et al., 2013; Riddick et al., 2014) as well as the dependence on emission from fertilizer on soil type as shown by the CHIMERE model (Hamaoui-Laguel et al., 2014). These initiatives are currently being addressed by the ECLAIRE project (http://www.eclaire-fp7.eu/), which focuses on climate-driven emissions (BVOCs and ammonia) as suggested by the latest IPCC report (2013), which calls for more studies on the feedback mechanisms between climate and air quality.

The Supplement related to this article is available online at doi:10.5194/bgd-12-2021-2015-supplement.

Acknowledgements. The study received support from the Polish National Science through projects no. UMO-2013/09/B/ST10/00594 and UMO-2011/03/B/ST10/06226. Preparation of the meteorological data was carried out at the Wrocław Centre for Networking and Supercomputing (http://www.wcss.wroc.pl) (grant no. 170).

References

Aas, W., Tsyro, S., Bieber, E., Bergström, R., Ceburnis, D., Ellermann, T., Fagerli, H., Frölich, M., Gehrig, R., Makkonen, U., Nemitz, E., Otjes, R., Perez, N., Perrino, C., Prévôt, A. S. H., Putaud, J.-P., Simpson, D., Spindler, G., Vana, M., and Yttri, K. E.: Lessons learnt from the first EMEP intensive measurement periods, Atmos. Chem. Phys., 12, 8073–8094, doi:10.5194/acp-12-8073-2012, 2012.

Anderson, N., Strader, R., and Davidson, C.: Airborne reduced nitrogen: ammonia emissions from agriculture and other sources, Environ. Int., 29, 277–86, doi:10.1016/S0160-4120(02)00186-1, 2003.

Asman, W. A. H., Sutton, M. A., and Schjorring, J. K.: Ammonia: emission, atmospheric transport and deposition, New Phytol., 139, 27–48, doi:10.1046/j.1469-8137.1998.00180.x, 1998.

Baklanov, A., Schlünzen, K., Suppan, P., Baldasano, J., Brunner, D., Aksoyoglu, S., Carmichael, G., Douros, J., Flemming, J., Forkel, R., Galmarini, S., Gauss, M., Grell, G., Hirtl, M., Joffre, S., Jorba, O., Kaas, E., Kaasik, M., Kallos, G., Kong, X., Korsholm, U., Kurganskiy, A., Kushta, J., Lohmann, U., Mahura, A., Manders-Groot, A., Maurizi, A., Moussiopoulos, N., Rao, S. T., Savage, N., Seigneur, C., Sokhi, R. S., Solazzo, E., Solomos, S., Sørensen, B., Tsegas, G., Vignati, E., Vogel, B., and Zhang, Y.: Online coupled regional meteorology chemistry models in Europe: current status and prospects, Atmos. Chem. Phys., 14, 317–398, doi:10.5194/acp-14-317-2014, 2014.

Banzhaf, S., Schaap, M., Wichink Kruit, R. J., Denier van der Gon, H. A. C., Stern, R., and Builtjes, P. J. H.: Impact of emission changes on secondary inorganic aerosol episodes across Germany, Atmos. Chem. Phys., 13, 11675–11693, doi:10.5194/acp-13-11675-2013, 2013.

Barrett, K.: Oceanic ammonia emissions in Europe and their transboundary fluxes, Atmos. Environ., 32, 381–391, doi:10.1016/S1352-2310(97)00279-3, 1998.

Bash, J. O., Cooter, E. J., Dennis, R. L., Walker, J. T., and Pleim, J. E.: Evaluation of a regional air-quality model with bidirectional NH_3 exchange coupled to an agroecosystem model, Biogeosciences, 10, 1635–1645, doi:10.5194/bg-10-1635-2013, 2013.

Bouwman, A. F., Lee, D. S., Asman, W. A. H., Dentener, F. J., Van Der Hoek, K. W., and Olivier, J. G. J.: A global high-resolution emission inventory for ammonia, Global Biogeochem. Cy., 11, 561–587, doi:10.1029/97GB02266, 1997.

David, M., Loubet, B., Cellier, P., Mattsson, M., Schjoerring, J. K., Nemitz, E., Roche, R., Riedo, M., and Sutton, M. A.: Ammonia sources and sinks in an intensively managed grassland canopy, Biogeosciences, 6, 1903–1915, doi:10.5194/bg-6-1903-2009, 2009.

De Meij, A., Thunis, P., Bessagnet, B., and Cuvelier, C.: The sensitivity of the CHIMERE model to emissions reduction scenarios on air quality in Northern Italy, Atmos. Environ., 43, 1897–1907, doi:10.1016/j.atmosenv.2008.12.036, 2009.

Dore, A. J., Vieno, M., Fournier, N., Weston, K. J., and Sutton, M. A.: Development of a new wind-rose for the British Isles using radiosonde data, and application to an atmospheric transport model, Q. J. Roy. Meteor. Soc., 132, 2769–2784, doi:10.1256/qj.05.198, 2006.

Dragosits, U., Sutton, M. A., Place, C. J., and Bayley, A. A.: Modelling the spatial distribution of agricultural ammonia emissions in the UK, Environ. Pollut., 102, 195–203, doi:10.1016/S0269-7491(98)80033-X, 1998.

Duyzer, J.: Dry deposition of ammonia and ammonium aerosols over heathland, J. Geophys. Res., 99, 18757, doi:10.1029/94JD01210, 1994.

Emmett, B. A.: Nitrogen saturation of terrestrial ecosystems: some recent findings and their implications for our conceptual framework, Water Air Soil Pollut., 7, 99–109, 2007.

Flechard, C. R., Massad, R.-S., Loubet, B., Personne, E., Simpson, D., Bash, J. O., Cooter, E. J., Nemitz, E., and Sutton, M. A.: Advances in understanding, models and parameterizations of biosphere-atmosphere ammonia exchange, Biogeosciences, 10, 5183–5225, doi:10.5194/bg-10-5183-2013, 2013.

Fournier, N., Dore, A. J., Vieno, M., Weston, K. J., Dragosits, U., and Sutton, M. A.: Modelling the deposition of atmospheric oxidised nitrogen and sulphur to the United Kingdom using a multi-layer long-range transport model, Atmos. Environ., 38, 683–694, doi:10.1016/j.atmosenv.2003.10.028, 2004.

Fowler, D.: Regional mass budgets of oxidized and reduced nitrogen and their relative contribution to the N inputs of sensitive ecosystems, Environ. Pollut., 102, 337–342, 1998.

Geels, C., Andersen, H. V., Ambelas Skjøth, C., Christensen, J. H., Ellermann, T., Løfstrøm, P., Gyldenkærne, S., Brandt, J., Hansen, K. M., Frohn, L. M., and Hertel, O.: Improved modelling of atmospheric ammonia over Denmark using the coupled modelling system DAMOS, Biogeosciences, 9, 2625–2647, doi:10.5194/bg-9-2625-2012, 2012.

Guevara, M., Martínez, F., Arévalo, G., Gassó, S., and Baldasano, J. M.: An improved system for modelling Spanish emissions: HERMESv2.0, Atmos. Environ., 81, 209–221, doi:10.1016/j.atmosenv.2013.08.053, 2013.

Gyldenkærne, S.: A dynamical ammonia emission parameterization for use in air pollution models, J. Geophys. Res., 110, D07108, doi:10.1029/2004JD005459, 2005.

Hamaoui-Laguel, L., Meleux, F., Beekmann, M., Bessagnet, B., Génermont, S., Cellier, P., and Létinois, L.: Improving ammonia emissions in air quality modelling for France, Atmos. Environ., 92, 584–595, doi:10.1016/j.atmosenv.2012.08.002, 2014.

Hansen, K., Sørensen, L. L., Hertel, O., Geels, C., Skjøth, C. A., Jensen, B., and Boegh, E.: Ammonia emissions from deciduous forest after leaf fall, Biogeosciences, 10, 4577–4589, doi:10.5194/bg-10-4577-2013, 2013.

BGD

12, 2021–2061, 2015

Understanding emissions of ammonia from buildings and fertilizer use

M. Werner et al.

Hellsten, S., Dragosits, U., Place, C. J., Vieno, M., Dore, A. J., Misselbrook, T. H., Tang, Y. S., and Sutton, M. A.: Modelling the spatial distribution of ammonia emissions in the UK, Environ. Pollut., 154, 370–9, doi:10.1016/j.envpol.2008.02.017, 2008.
Hertel, O., Skjøth, C. A., Reis, S., Bleeker, A., Harrison, R. M., Cape, J. N., Fowler, D., Skiba, U., Simpson, D., Jickells, T., Kulmala, M., Gyldenkærne, S., Sørensen, L. L., Erisman, J. W., and Sutton, M. A.: Governing processes for reactive nitrogen compounds in the European atmosphere, Biogeosciences, 9, 4921–4954, doi:10.5194/bg-9-4921-2012, 2012.
Hettelingh, J. P., Posch, M., and Slootweg, J.: Progress in the Modelling of Critical Thresholds and Dynamic Modelling, incl.
Hong, S.-Y., Noh, Y., and Dudhia, J.: A new vertical diffusion package with an explicit treatment of entrainment processes, Mon. Weather Rev., 134, 2318–2341, 2006.
Iacono, M. J., Delamere, J. S., Mlawer, E. J., Shephard, M. W., Clough, S. A., and Collins, W. D.: Radiative forcing by long-lived greenhouse gases: calculations with the AER radiative transfer models, J. Geophys. Res., 113, D13103, doi:10.1029/2008JD009944, 2008.
Jones, M. L. M., Norris, D., Hall, J., and Petit, S.: Developing an indicator-modelling approach to forecast changes in nitrogen critical load exceedance across Europe arising from agricultural reform, Ecol. Indic., 11, 16–26, doi:10.1016/j.ecolind.2009.06.005, 2011a.
Jones, M. L. M., Norris, D., Hall, J., and Petit, S.: Developing an indicator-modelling approach to forecast changes in nitrogen critical load exceedance across Europe arising from agricultural reform, Ecol. Indic., 11, 16–26, doi:10.1016/j.ecolind.2009.06.005, 2011b.
Kain, J. S.: The Kain–Fritsch Convective Parameterization: an Update, J. Appl. Meteorol., 43, 170–181, 2004.
Klimont, Z. and Brink, C.: Modelling of Emissions of Air Pollutants and Greenhouse Gases from Agricultural Sources in Europe, Ina. Rep., R. Minist. Environ. Oslo, Norw., 2004.
Kryza, M., Werner, M., Błaś, M., Dore, A. J., and Sobik, M.: The effect of emission from coal combustion in nonindustrial sources on deposition of sulfur and oxidized nitrogen in Poland., J. Air Waste Manag. Assoc., 60, 856–866, 2010.
Kryza, M., Dore, A. J., Błaś, M., and Sobik, M.: Modelling deposition and air concentration of reduced nitrogen in Poland and sensitivity to variability in annual meteorology, J. Environ. Manage., 92, 1225–1236, doi:10.1016/j.jenvman.2010.12.008, 2011.
Kryza, M., Werner, M., Dore, A. J., Błaś, M., and Sobik, M.: The role of annual circulation and precipitation on national scale deposition of atmospheric sulphur and nitrogen compounds., J. Environ. Manage., 109, 70–79, doi:10.1016/j.jenvman.2012.04.048, 2012.

Kryza, M., Mill, W., Dore, A. J., Werner, M., and Błaś, M.: Calculation of sulphur and nitrogen deposition with the frame model and assessment of the exceedance of critical loads in Poland, Ecol. Chem. Eng. S., 20, 279–290, doi:10.2478/eces-2013-0020, 2013a.

Kryza, M., Werner, M., Wałszek, K., and Dore, A. J.: Application and evaluation of the WRF model for high-resolution forecasting of rainfall – a case study of SW Poland, Meteorol. Z., 22, 595–601, doi:10.1127/0941-2948/2013/0444, 2013b.

Massad, R.-S., Nemitz, E., and Sutton, M. A.: Review and parameterisation of bi-directional ammonia exchange between vegetation and the atmosphere, Atmos. Chem. Phys., 10, 10359–10386, doi:10.5194/acp-10-10359-2010, 2010.

Mattsson, M., Herrmann, B., David, M., Loubet, B., Riedo, M., Theobald, M. R., Sutton, M. A., Bruhn, D., Neftel, A., and Schjoerring, J. K.: Temporal variability in bioassays of the stomatal ammonia compensation point in relation to plant and soil nitrogen parameters in intensively managed grassland, Biogeosciences, 6, 171–179, doi:10.5194/bg-6-171-2009, 2009.

Misselbrook, T. H., Sutton, M. A., and Scholefield, D.: A simple process-based model for estimating ammonia emissions from agricultural land after fertilizer applications, Soil Use Manag., 20, 365–372, doi:10.1111/j.1475-2743.2004.tb00385.x, 2006.

Mlawer, E. J., Taubman, S. J., Brown, P. D., Iacono, M. J., and Clough, S. A.: Radiative transfer for inhomogeneous atmospheres: RRTM, a validated correlated-k model for the longwave, J. Geophys. Res., 102, 16663, doi:10.1029/97JD00237, 1997.

Mues, A., Kuenen, J., Hendriks, C., Manders, A., Segers, A., Scholz, Y., Hueglin, C., Builtjes, P., and Schaap, M.: Sensitivity of air pollution simulations with LOTOS-EUROS to the temporal distribution of anthropogenic emissions, Atmos. Chem. Phys., 14, 939–955, doi:10.5194/acp-14-939-2014, 2014.

Nagel, H. D. and Gregor, H. D.: Derivation and mapping of critical loads for nitrogen and trends in their exceedance in Germany, Scient. World J., 1, 936–944, doi:10.1100/tsw.2001.330, 2001.

Olesen, J. E. and Plauborg, F.: MVTOOL version 1.10 for developing MARKVAND, Danish Institute of Plant Soil Science, Research Centre Foulum, 1995.

Oxley, T., Dore, A. J., ApSimon, H., Hall, J., and Kryza, M.: Modelling future impacts of air pollution using the multi-scale UK Integrated Assessment Model (UKIAM), Environ. Int., 61, 17–35, doi:10.1016/j.envint.2013.09.009, 2013.

Paulot, F., Jacob, D. J., Pinder, R. W., Bash, J. O., Travis, K., and Henze, D. K.: Ammonia emissions in the United States, European Union, and China derived by high-resolution inversion of ammonium wet deposition data: interpretation with a new agricultural emissions inventory (MASAGE_NH3), J. Geophys. Res.-Atmos., 119, 4343–4364, doi:10.1002/2013JD021130, 2014.

Reis, S., Pinder, R. W., Zhang, M., Lijie, G., and Sutton, M. A.: Reactive nitrogen in atmospheric emission inventories, Atmos. Chem. Phys., 9, 7657–7677, doi:10.5194/acp-9-7657-2009, 2009.

Riddick, S. N., Blackall, T. D., Dragosits, U., Daunt, F., Braban, C. F., Tang, Y. S., MacFarlane, W., Taylor, S., Wanless, S., and Sutton, M. A.: Measurement of ammonia emissions from tropical seabird colonies, Atmos. Environ., 89, 35–42, doi:10.1016/j.atmosenv.2014.02.012, 2014.

Seedorf, J., Hartung, J., Schröder, M., Linkert, K. H., Pedersen, S., Takai, H., Johnsen, J. O., Metz, J. H. M., Groot Koerkamp, P. W. G., Uenk, G. H., Phillips, V. R., Holden, M. R., Sneath, R. W., Short, J. L. L., White, R. P., and Wathes, C. M.: A survey of ventilation rates in livestock buildings in Northern Europe, J. Agric. Eng. Res., 70, 39–47, doi:10.1006/jaer.1997.0274, 1998a.

Seedorf, J., Hartung, J., Schröder, M., Linkert, K. H., Pedersen, S., Takai, H., Johnsen, J. O., Metz, J. H. M., Groot Koerkamp, P. W. G., Uenk, G. H., Phillips, V. R., Holden, M. R., Sneath, R. W., Short, J. L., White, R. P., and Wathes, C. M.: Temperature and moisture conditions in livestock buildings in Northern Europe, J. Agric. Eng. Res., 70, 49–57, doi:10.1006/jaer.1997.0284, 1998b.

Seinfeld, J. H. and Pandis, S. N.: Atmospheric Chemisty and Physics: From Air Pollution to Climate Change, John Wiley Sons Inc., New York, 2006.

Singles, R., Sutton, M. A., and Weston, K. J.: A multi-layer model to describe the atmospheric transport and deposition of ammonia in Great Britain, Atmos. Environ., 32, 393–399, doi:10.1016/S1352-2310(97)83467-X, 1998.

Skamarock, W. C. and Klemp, J. B.: A time-split nonhydrostatic atmospheric model for weather research and forecasting applications, J. Comput. Phys., 227, 3465–3485, doi:10.1016/j.jcp.2007.01.037, 2008.

Skjøth, C. A. and Geels, C.: The effect of climate and climate change on ammonia emissions in Europe, Atmos. Chem. Phys., 13, 117–128, doi:10.5194/acp-13-117-2013, 2013.

Skjøth, C. A., Hertel, O., Gyldenkærne, S., and Ellermann, T.: Implementing a dynamical ammonia emission parameterization in the large-scale air pollution model ACDEP, J. Geophys. Res., 109, D06306, doi:10.1029/2003JD003895, 2004.

Skjøth, C. A., Geels, C., Hvidberg, M., Hertel, O., Brandt, J., Frohn, L. M., Hansen, K. M., Hedegaard, G. B., Christensen, J. H., and Moseholm, L.: An inventory of tree species in Europe – an essential data input for air pollution modelling, Ecol. Modell., 217, 292–304, doi:10.1016/j.ecolmodel.2008.06.023, 2008.

Skjøth, C. A., Geels, C., Berge, H., Gyldenkærne, S., Fagerli, H., Ellermann, T., Frohn, L. M., Christensen, J., Hansen, K. M., Hansen, K., and Hertel, O.: Spatial and temporal variations in ammonia emissions – a freely accessible model code for Europe, Atmos. Chem. Phys., 11, 5221–5236, doi:10.5194/acp-11-5221-2011, 2011.

Sørensen, L. L., Hertel, O., Skjøth, C. A., Lund, M., and Pedersen, B.: Fluxes of ammonia in the coastal marine boundary layer, Atmos. Environ., 37, 167–177, doi:10.1016/S1352-2310(03)00247-4, 2003.

Stevens, C. J., Dise, N. B., Mountford, J. O., and Gowing, D. J.: Impact of nitrogen deposition on the species richness of grasslands, Science, 303, 1876–1879, doi:10.1126/science.1094678, 2004.

Stoelinga., M.: A Users' Guide to RIP Version 4: a Program for Visualizing Mesoscale Model Output, Univ. Washingt., 2008.

Sutton, M. A., Burkhardt, J. K., Guerin, D., Nemitz, E., and Fowler, D.: Development of resistance models to describe measurements of bi-directional ammonia surface–atmosphere exchange, Atmos. Environ., 32, 473–480, doi:10.1016/S1352-2310(97)00164-7, 1998.

Sutton, M. A., Nemitz, E., Theobald, M. R., Milford, C., Dorsey, J. R., Gallagher, M. W., Hensen, A., Jongejan, P. A. C., Erisman, J. W., Mattsson, M., Schjoerring, J. K., Cellier, P., Loubet, B., Roche, R., Neftel, A., Hermann, B., Jones, S. K., Lehman, B. E., Horvath, L., Weidinger, T., Rajkai, K., Burkhardt, J., Löpmeier, F. J., and Daemmgen, U.: Dynamics of ammonia exchange with cut grassland: strategy and implementation of the GRAMINAE Integrated Experiment, Biogeosciences, 6, 309–331, doi:10.5194/bg-6-309-2009, 2009.

Sutton, M. A., Reis, S., Riddick, S. N., Dragosits, U., Nemitz, E., Theobald, M. R., Tang, Y. S., Braban, C. F., Vieno, M., Dore, A. J., Mitchell, R. F., Wanless, S., Daunt, F., Fowler, D., Blackall, T. D., Milford, C., Flechard, C. R., Loubet, B., Massad, R., Cellier, P., Personne, E., Coheur, P. F., Clarisse, L., Van Damme, M., Ngadi, Y., Clerbaux, C., Skjøth, C. A., Geels, C., Hertel, O., Wichink Kruit, R. J., Pinder, R. W., Bash, J. O., Walker, J. T., Simpson, D., Horváth, L., Misselbrook, T. H., Bleeker, A., Dentener, F., and de Vries, W.: Towards a climate-dependent paradigm of ammonia emission and deposition., Philos. Trans. R. Soc. Lond. B, 368, 20130166, doi:10.1098/rstb.2013.0166, 2013.

Szymanowski, M., Kryza, M., and Spallek, W.: Regression-based air temperature spatial prediction models: an example from Poland, Meteorol. Z., 22, 577–585, doi:10.1127/0941-2948/2013/0440, 2013.

Tao, W.-K., Simpson, J., and McCumber, M.: An ice-water saturation adjustment, Mon. Weather Rev., 117, 231–235, 1989.

Theobald, M. R., Bealey, W. J., Tang, Y. S., Vallejo, A., and Sutton, M. A.: A simple model for screening the local impacts of atmospheric ammonia., Sci. Total Environ., 407, 6024–6033, doi:10.1016/j.scitotenv.2009.08.025, 2009.

van Grinsven, H. J. M., ten Berge, H. F. M., Dalgaard, T., Fraters, B., Durand, P., Hart, A., Hofman, G., Jacobsen, B. H., Lalor, S. T. J., Lesschen, J. P., Osterburg, B., Richards, K. G., Techen, A.-K., Vertès, F., Webb, J., and Willems, W. J.: Management, regulation and environmental impacts of nitrogen fertilization in northwestern Europe under the Nitrates Directive; a benchmark study, Biogeosciences, 9, 5143–5160, doi:10.5194/bg-9-5143-2012, 2012.

Van Pul, W. A. J., van Jaarsveld, J. A., Vellinga, O. S., van den Broek, M., and Smits, M. C. J.: The VELD experiment: an evaluation of the ammonia emissions and concentrations in an agricultural area, Atmos. Environ., 42, 8086–8095, doi:10.1016/j.atmosenv.2008.05.069, 2008.

Vieno, M., Dore, A. J., Stevenson, D. S., Doherty, R., Heal, M. R., Reis, S., Hallsworth, S., Tarrason, L., Wind, P., Fowler, D., Simpson, D., and Sutton, M. A.: Modelling surface ozone during the 2003 heat-wave in the UK, Atmos. Chem. Phys., 10, 7963–7978, doi:10.5194/acp-10-7963-2010, 2010.

Werner, M., Kryza, M., and Dore, A. J.: Differences in the spatial distribution and chemical composition of PM_{10} between the UK and Poland, Environ. Model. Assess., 19, 179–192, doi:10.1007/s10666-013-9384-0, 2014a.

Werner, M., Kryza, M., Skjøth, C. A., Wałaszek, K., Dore, A. J., and Ojrzyńska, H.: Aerosol-radiation feedback and PM_{10} air concentrations over Poland, Pure abd Appl. Geophys., in revision, 2014b.

Wichink Kruit, R. J., Schaap, M., Sauter, F. J., van Zanten, M. C., and van Pul, W. A. J.: Modeling the distribution of ammonia across Europe including bi-directional surface–atmosphere exchange, Biogeosciences, 9, 5261–5277, doi:10.5194/bg-9-5261-2012, 2012.

Xu, L. and Penner, J. E.: Global simulations of nitrate and ammonium aerosols and their radiative effects, Atmos. Chem. Phys., 12, 9479–9504, doi:10.5194/acp-12-9479-2012, 2012.

Żmudzka, E.: Wieloletnie zmiany zasobów termicznych w okresie wegetacyjnym i aktywnego wzrostu roślin w Polsce, Woda-Środowisko-Obszary Wiej., T. 12, z. 2, 377–389, 2012.

Table 1. The functions describing the temporal variation in NH_3 emissions from various activities*.

Function	Description	Required meteorological parameters*
Fct_1	Animal houses with forced ventilation	W_i, T_i
Fct_2	Open animal houses	W_i, T_i
Fct_3	Manure storage	W_i, T_i
Fct_8	Spring application of manure on bare soil	W_{corr}, T_{corr}
Fct_9	Application of manure on crops	W_{corr}, T_{corr}
Fct_{10}	Summer application of manure	W_{corr}, T_{corr}
Fct_{11}	Autumn application of manure	W_{corr}, T_{corr}
Fct_{12}	Spring application of fertilizers	W_{corr}, T_{corr}
Fct_{13}	Summer application of fertilizers	W_{corr}, T_{corr}
Fct_{14}	Emission related to grassing cattle	W_{corr}, T_{corr}
Fct_{15}	Emission related to ammonia-treated straw	W_{corr}, T_{corr}

* Functions Fct_4–Fct_7 have not been simulated in this study (Fct_4 – winter crops; Fct_5 – spring crops; Fct_6 – later spring crops; Fct_7 – grass)

Table 2. The emission scenarios used in this study.

Scenario*	Description
DEFAULT (1)	A default emission distribution that matches the European-wide default settings in the ammonia emission model, based on the original Danish model (Skjøth et al., 2011).
NOFERT (2)	An emission scenario that excludes application of manure and mineral fertilizer.
FLAT (3)	The existing emission method (no temporal variations) used in WRF-Chem over Poland (Werner et al., 2014a, b).
POLREGUL (4)	A scenario that takes into account Polish infrastructure and current and less regulation compared to Denmark (Klimont and Brink, 2004).

* Scenarios DEFAULT, NOFERT and POLREGUL were prepared with the ammonia emission model (Skjøth et al., 2011) described in Sect. 2.1.

BGD
12, 2021–2061, 2015

Table 3. Relative distribution of the total NH_3 emission from the agricultural activities in Poland as defined by Fct_1–Fct_{15}. Poland default – distribution based on European-wide default settings; Poland scenario – distribution based on Polish infrastructure and regulations.

Name	Fct_1	Fct_2	Fct_3	Fct_8	Fct_9	Fct_{10}	Fct_{11}	Fct_{11a}	Fct_{12}	Fct_{13}	Fct_{14}	Fct_{15}
Poland default	0.20	0.09	0.07	0.09	0.09	0.00	0.05	0.05	0.28	0.03	0.05	0.01
Poland scenario	0.20	0.09	0.07	0.07	0.05	0.02	0.07	0.07	0.10	0.20	0.05	0.01

BGD
12, 2021–2061, 2015

Table 4. Domain-wide error statistics for 2 m temperature (T2) and 10 m wind speed (W10) over Poland for 2010.

	ME	MAE	IOA
T2	−0.68 K	1.79 K	0.99
W10	0.16 m s^{-1}	1.29 m s^{-1}	0.84

BGD
12, 2021–2061, 2015

Table 5. FRAME model results – error statistics for the individual sites (mean from 12 months).

Statistic	Run	Rzecin	Jarczew	Łeba	Śnieżka	Diabla Góra
ME	DEFAULT	−0.32	1.44	0.26	0.56	−0.02
($\mu g\, m^{-3}$)	NOFERT	−0.76	−0.50	−0.14	0.21	−0.47
	FLAT	−0.34	0.31	0.00	0.13	−0.13
	POLREGUL	−0.36	1.30	0.24	0.51	−0.07
MAE	DEFAULT	0.68	1.75	0.48	0.56	0.74
($\mu g\, m^{-3}$)	NOFERT	0.76	0.55	0.18	0.21	0.49
	FLAT	0.63	0.62	0.24	0.16	0.25
	POLREGUL	0.39	1.66	0.33	0.51	0.68
R	DEFAULT	0.48	0.55	0.06	0.38	−0.28
(unitless)	NOFERT	0.92	0.81	0.64	0.43	−0.80
	FLAT	0.02	0.72	−0.18	0.14	0.06
	POLREGUL	0.85	0.84	0.65	0.65	−0.55

BGD
12, 2021–2061, 2015

Table 6. FRAME error results – error statistics from all sites for summer (III–X) and winter (XI–II) period. Unit for ME and MAE is $\mu g\,m^{-3}$; R is unitless.

	DEFAULT			NOFERT			FLAT			POLREGUL		
	year	III–X	XI–II	year	III–X	XI–II	year	III–X	XI–II	year	III–X	XI–II
ME	0.23	0.70	−0.25	−0.31	−0.36	−0.25	0.07	−0.12	0.25	0.16	0.65	−0.32
MAE	0.54	0.83	0.25	0.31	0.36	0.25	0.23	0.21	0.25	0.50	0.68	0.32
R	0.48	0.21	0.75	0.72	0.70	0.75	0.26	0.04	0.48	0.01	0.73	−0.71

BGD
12, 2021–2061, 2015

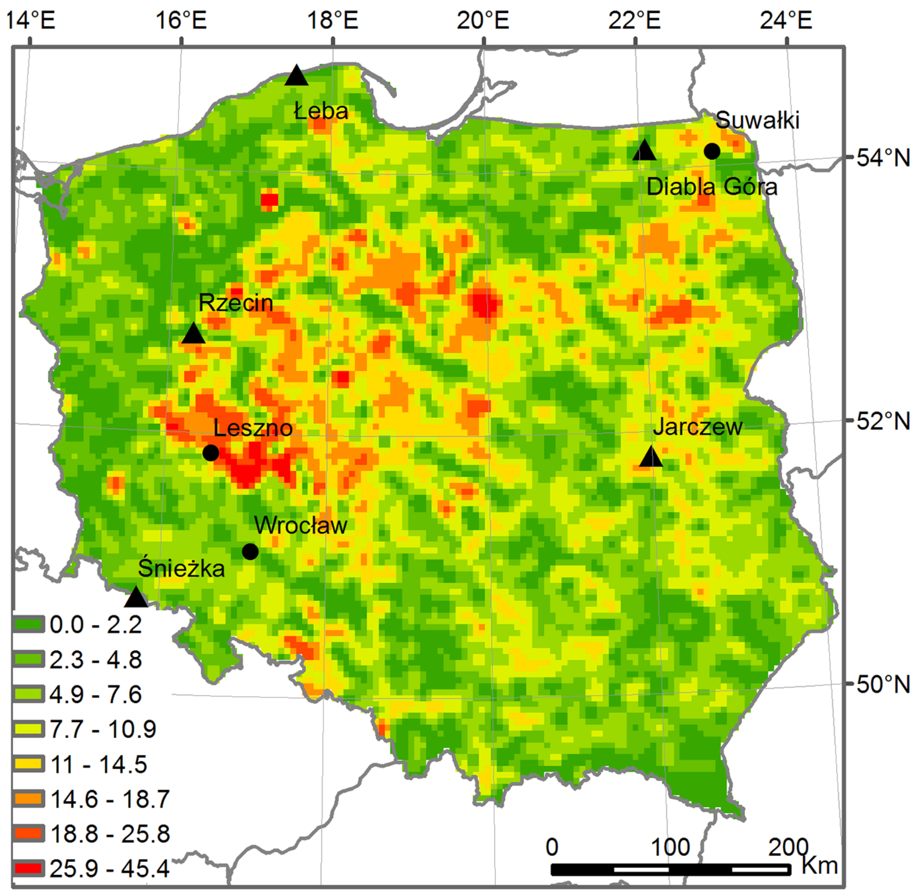

Figure 1. Total annual emission of NH_3 in 2010 [$kg\,ha^{-1}\,year^{-1}$]. NH_3 measurement sites indicated by triangles. Additional locations discussed in the paper indicated by circles (Wrocław, Leszno, Suwałki).

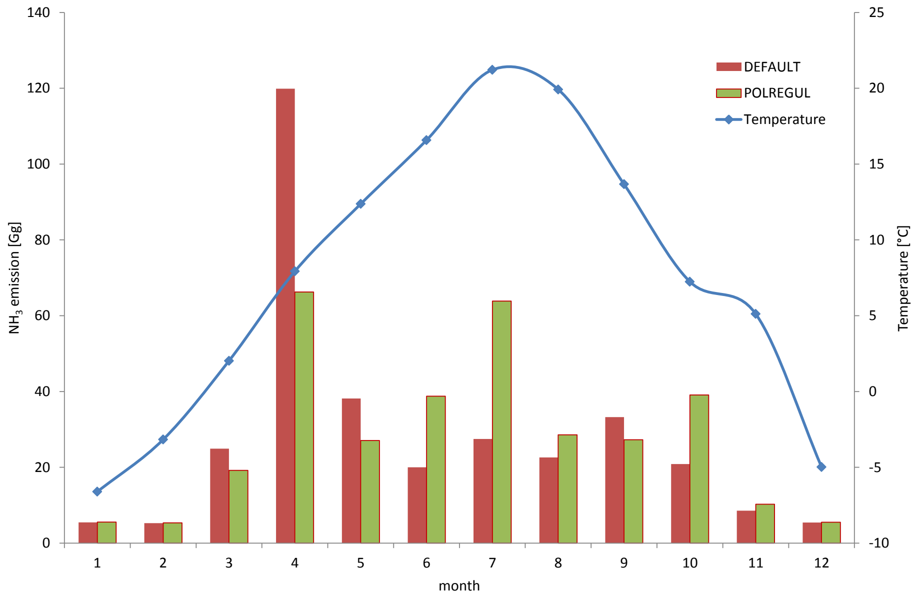

Figure 2. Monthly emission of NH_3 for DEFAULT and POLREGUL run and average temperature in 2010.

BGD

12, 2021–2061, 2015

Understanding emissions of ammonia from buildings and fertilizer use

M. Werner et al.

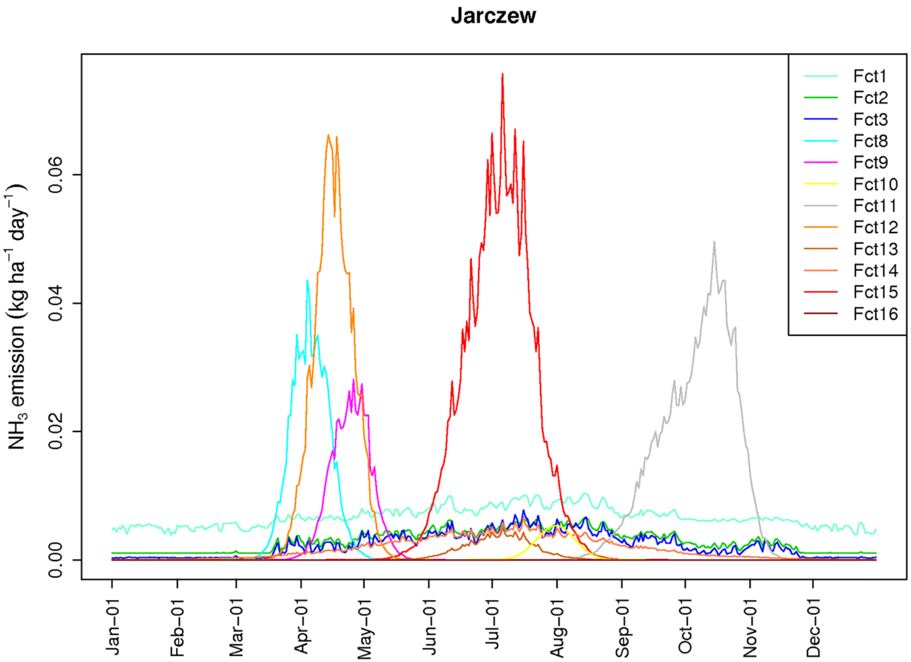

Figure 3. Time series of the seasonal variation in emission (POLREGUL run) for various agricultural emission categories in Jarczew (functions (Fct) described in Table 1).

BGD
12, 2021–2061, 2015

Understanding emissions of ammonia from buildings and fertilizer use

M. Werner et al.

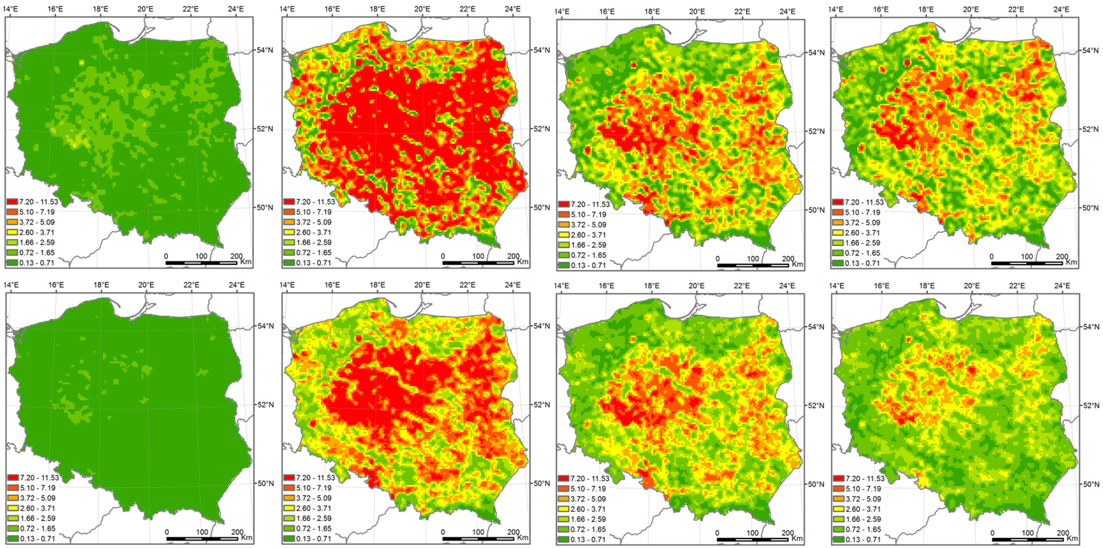

Figure 4. Top: spatial distribution of NH_3 emissions over Poland for 15 February, 15 April, 15 June and 15 September 2010 at 12:00–15:00 UTC [$g\,ha^{-1}\ 3\,h^{-1}$]. Bottom: monthly mean ammonia concentrations calculated with the FRAME model (POLREGUL) for February, April, June and September 2010.

BGD
12, 2021–2061, 2015
Understanding emissions of ammonia from buildings and fertilizer use
M. Werner et al.

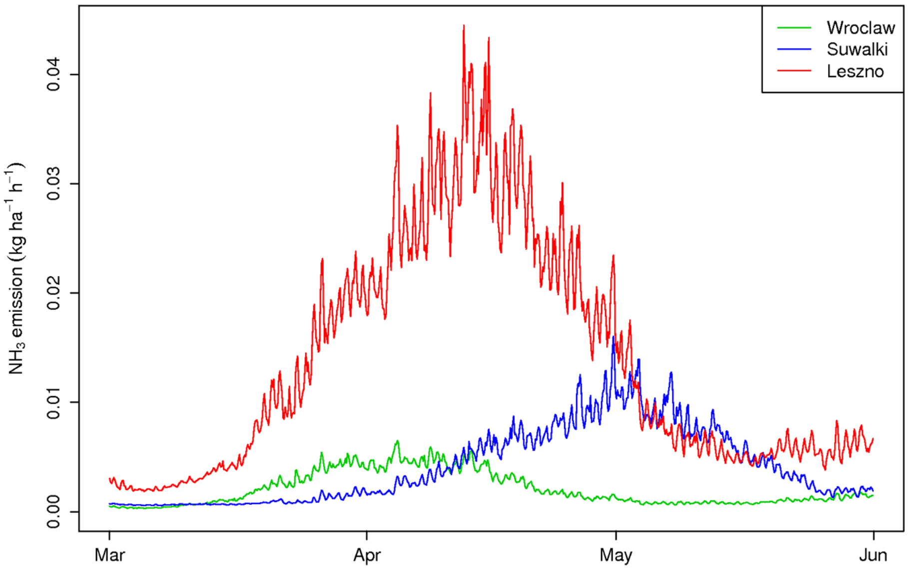

Figure 5. The hourly variation in simulated NH_3 emissions for POLREGUL scenario. Data from March to May for three locations in Poland (Wrocław, Suwałki and Leszno).

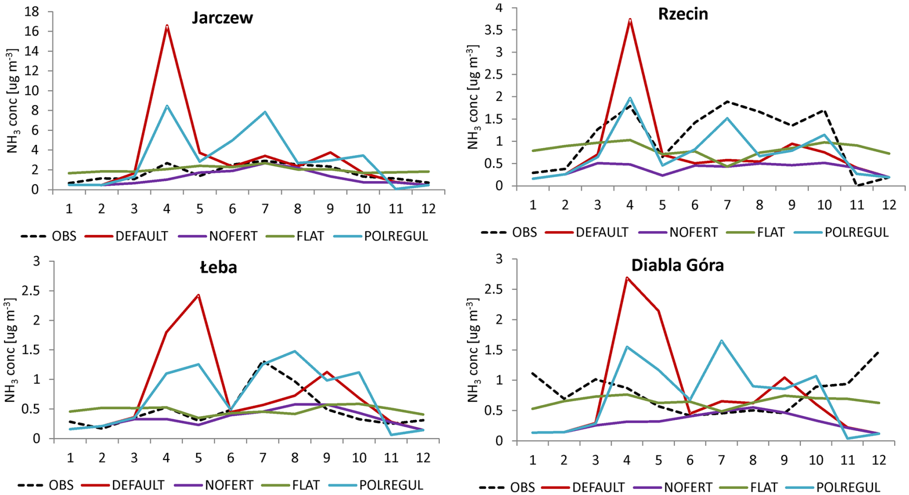

Figure 6. Time series of modelled and measured NH_3 concentrations for 2010.

BGD
12, 2021–2061, 2015

Understanding emissions of ammonia from buildings and fertilizer use

M. Werner et al.

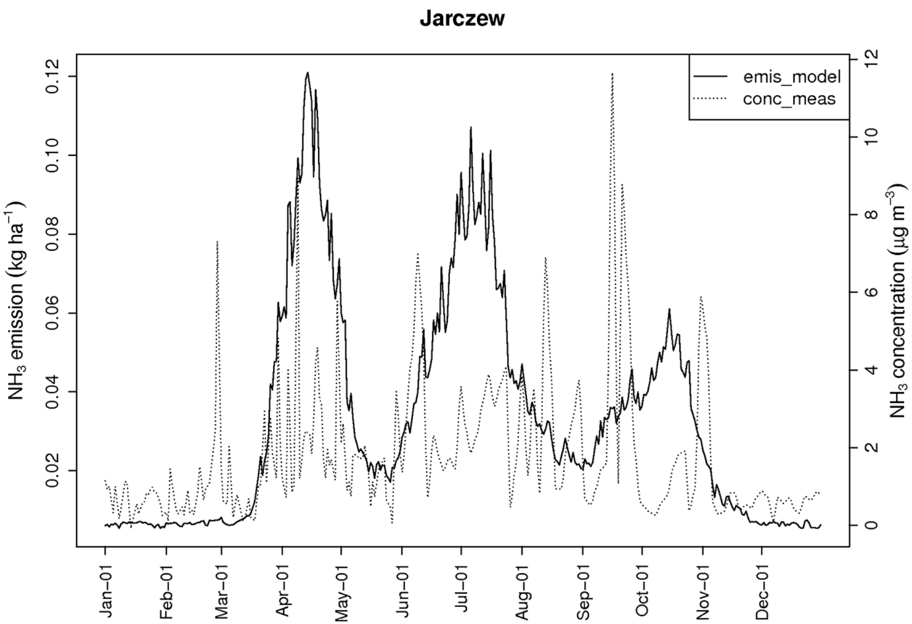

Figure 7. Modelled emission and measured concentration for the Jarczew station.

BGD
12, 2021–2061, 2015

Understanding emissions of ammonia from buildings and fertilizer use

M. Werner et al.

Title Page
Abstract Introduction
Conclusions References
Tables Figures
◀◀ ▶▶
◀ ▶
Back Close
Full Screen / Esc
Printer-friendly Version
Interactive Discussion

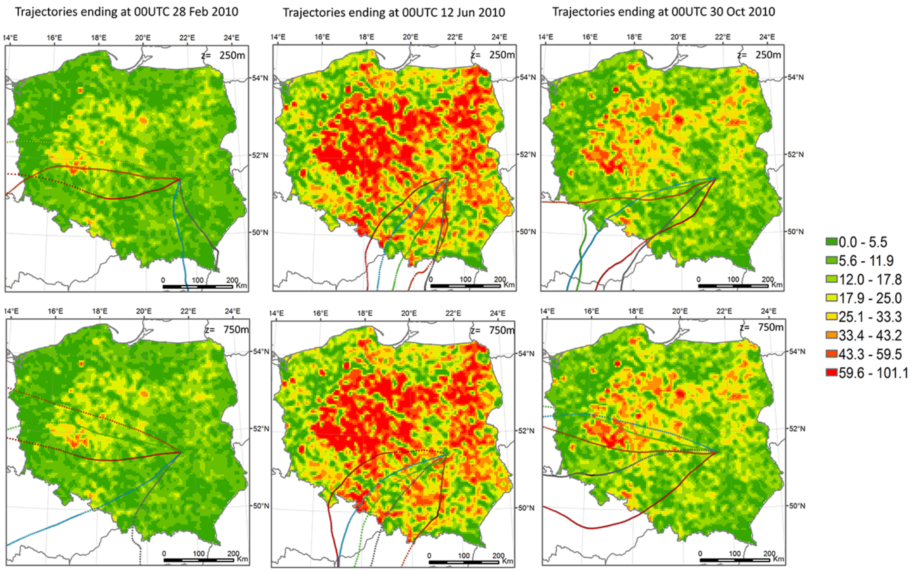

Figure 8. Thirty-six-hour backward trajectories ending in Jarczew during episodes (25–27 February 2010, 09–11 June 2010, 10–29 October 2010) with high NH_3 measured concentrations. The first trajectory (grey) starts at 12:00 of the first day of each episode, and then starts every 6 h, and are presented in the following colours: blue, green, orange and red. Spatial distribution of modelled ammonia emission during the episodes (unit: $g\,ha^{-1}\,48\,h^{-1}$).